

Article

# Thermodynamic Model of a Gas Turbine Considering Atmospheric Conditions and Position of the IGVs

Tarik Boushaki \* and Kacem Mansouri

Laboratoire d'Énergétique, Mécanique et Ingénieries (LEMI), Département de Génie Mécanique, Faculté de Technologie, Université M'hamed BOUGARA de Boumerdes (UMBB), Boumerdes 35000, Algeria

\* Correspondence: t.boushaki@univ-boumerdes.dz

**Abstract:** Gas turbines are widely used in power generation due to their efficiency, flexibility, and low environmental impact. Modeling, especially in thermodynamics, is crucial for the designer and operator of a gas turbine. An advanced and rigorous thermodynamic model is essential to accurately predict the performance of a gas turbine under on-design operating conditions, off-design or failure. Such models not only improve understanding of internal processes but also optimize performance and reliability in a wide variety of operational scenarios. This article presents the development of a thermodynamic model simulating the off-design performance of a gas turbine. The mathematical relationships established in this model allow for quick calculations while requiring a limited amount of data. Only nominal data are required, and some additional data are needed to calibrate the model on the turbine under study. A key feature of this model is the development of an innovative relationship that allows direct calculation of the mass flow of air entering the turbine and, thus, the performances of the turbine according to atmospheric conditions (such as pressure, temperature, and relative humidity) and the position of the compressor inlet guide vanes (IGV). The results of the simulations, obtained using code implemented in MATLAB (R2014a), demonstrate the efficiency of the model compared to experimental data. Indeed, the model relationships exhibit high determination coefficients ( $R^2 > 0.95$ ) and low root mean square errors (RMSE). Specifically, the simulation results for the air mass flow rate demonstrate a very high determination coefficient ( $R^2 = 0.9796$ ) and a low root mean square error (RMSE = 0.0213).



Academic Editor: Sébastien Poncet

Received: 9 December 2024

Revised: 1 February 2025

Accepted: 5 February 2025

Published: 7 February 2025

**Citation:** Boushaki, T.; Mansouri, K. Thermodynamic Model of a Gas Turbine Considering Atmospheric Conditions and Position of the IGVs. *Thermo* **2025**, *5*, 5. <https://doi.org/10.3390/thermo5010005>

**Copyright:** © 2025 by the authors. Licensee MDPI, Basel, Switzerland. This article is an open access article distributed under the terms and conditions of the Creative Commons Attribution (CC BY) license (<https://creativecommons.org/licenses/by/4.0/>).

**Keywords:** gas turbine; gas turbine performance; impact on performance; inlet guide vane; thermodynamic model; off-design

## 1. Introduction

Gas turbines play a key role in various industrial sectors, such as power generation and aeronautics, because they provide high specific power and ample operational flexibility. However, their performance is highly dependent on ambient atmospheric conditions, particularly temperature, pressure, and relative humidity, as well as the position of the IGV, which regulates the flow of air entering the turbine. Numerous studies have examined the impact of these factors and developed thermodynamic models to improve the accuracy of performance predictions, thus contributing to more efficient management of turbines in various environments.

Walsh and P. Fletcher [1] comprehensively analyze turbine operating principles and performance factors, including the impacts of ambient conditions and IGV settings. The authors provide analytical tools and simulation data to evaluate turbine performance in

different operational contexts. A. A. Sammour et al. [2] explored the influence of ambient air temperature and humidity on gas turbine performance. The study shows that net power decreases from 93.3 MW at 15 °C to 70 MW at 45 °C, while output decreases from 32.32% at 5 °C to 28.3% at 30 °C. W. H. S. Alaabidy [3] studied the operation of gas turbines in hot, dusty conditions typical of the Arab Gulf countries. The study shows reduced efficiency, lifetime, and higher maintenance costs due to ambient temperature and air quality. T. K. Ibrahim et al. [4] and A. Mousafarash and M. Ameri [5] conducted a gas turbine's energy and exergetic analysis. The results of both studies show the negative effect of high ambient temperatures on energy and exergy yields. A. Gonzalez-Díaz et al. [6] assessed the impact of ambient temperature on the performance of a natural gas combined cycle equipped with post-combustion CO<sub>2</sub> capture in Mexico. Results show that when the ambient temperature goes from 15 °C to 45 °C, the DC efficiency decreases from 50.95% to 48.01%, and the power decreases from 676.3 MW to 530 MW. M. B. Hashmi et al. [7] studied the effects of IGV fouling and increased inlet air temperature on the performance of a three-shaft gas turbine. Using a simulation model developed with GasTurb 12, the researchers demonstrated significant performance degradation, with power and thermal efficiency decreases of 21.09% and 7.92%, respectively, due to fouling and high air temperatures.

Fang Jihui et al. [8] investigated the influence of the degree of the IGV opening on the efficiency of the Mitsubishi F4 gas turbine compressor. The study reveals the impact of the degree of openness on compressor capacity and efficiency, particularly under variable ambient conditions. M. Ricci et al. [9] explored two operational strategies, including IGVs, to avoid gas turbine shutdowns during low power demand. Three-dimensional CFD analysis shows the existence of effective solutions to improve off-design performance. Wei Zhu et al. [10] proposed a new method to improve the partial load performance of gas turbines by adjusting the compressor inlet air temperature and opening of the IGV. The results suggest that proper regulation improves gas turbine efficiency and stability. O. Purba and F. Zhultriza [11] discussed the application of the IGV opening track in a combined cycle, emphasizing partial load efficiency. The results indicate that the implementation of LMI leads to an improvement in combined cycle efficiency of 1.5% of the efficiency during partial load operations. Z. Wang and L. Duan [12] discussed the thermo-economic optimization of heat recovery steam generators (HRSG) in gas turbine combined cycles. The results show that a strategy for using the IGV is necessary to reduce electricity production costs.

Numerous studies have explored how atmospheric conditions and the inlet guide vane (IGV) opening angle affect gas turbine performance. Most analyses utilize measured operational data to assess the influence of these parameters on performance. In some cases, researchers employ thermodynamic models or simulation software, such as GasTurb or EES, to simulate performance under various conditions. However, these simulations often require the air mass flow rate as an input, which must be predetermined.

Few studies have focused on modeling air mass flow as a function of atmospheric conditions, with the majority assuming air behaves as a perfect gas. Additionally, limited research has investigated the relationship between air mass flow and the IGV opening angle. Notably, no existing studies have simultaneously modeled air mass flow based on both atmospheric conditions and IGV positioning.

The proposed model addresses this gap by enabling the direct simulation of air mass flow rate. Consequently, the output power and thermal efficiency of gas turbines can be accurately calculated using atmospheric conditions and the inlet guide vane (IGV) opening angle as direct inputs.

The model's accuracy is further enhanced by modeling the relationship between the air volumetric flow rate and the opening angle of IGV using a second-degree polynomial function instead of a simple proportional relationship. This approach provides a more

accurate representation of volumetric flow behavior, enhancing the model's predictive accuracy. Finally, the proposed model offers rapid and efficient computation of results, ensuring both accuracy and practicality.

## 2. Combined Cycle Description

The combined gas–steam cycle combines a Brayton (gas turbine) cycle with a Rankine (steam turbine) cycle. This combination allows the heat of the turbine exhaust gas to be exploited, thus using the energy supplied by the fuel more efficiently and increasing overall efficiency. The gas turbine operates based on the thermodynamic Brayton cycle. Ambient air is first drawn in and compressed by an axial compressor, increasing its pressure and temperature. The compressed air is then mixed with fuel, typically natural gas, in a combustion chamber. The combustion process generates hot gases, often exceeding 1200 °C. These hot gases expand through the gas turbine, converting thermal energy into mechanical energy. The turbine drives an alternator, enabling the generation of electricity. Instead of being released into the atmosphere, the burned gases, which are still at high temperatures (400–600 °C), are delivered to a heat recovery steam generator (HRSG), which harnesses the heat from the gases to create steam using heat exchangers. The steam produced by the HRSG feeds the steam cycle based on the thermodynamic Rankine cycle. This steam first relaxes in a steam turbine, and at the exit of the turbine, it is condensed in a condenser from which it comes out in a liquid state; the liquid water is then compressed by a pump and returned to the HRSG. The steam turbine produces surplus electricity, which improves overall efficiency (up to 60%) while reducing losses and emissions. The combined gas–steam cycle is an efficient and rather environmentally friendly technology for electricity generation. Currently, combined cycle power plants are widely used and represent a good solution for a gradual transition from fossil fuels to renewable energies.

Our study relates to the combined cycle power plant located at Cap Djenet in Algeria, with a capacity of 1131.1 MW under site conditions. The power plant essentially comprises three “single-shaft” units, Siemens SCC5-4000F 1S. Each unit comprises a Siemens SGT5-4000F gas turbine, a Siemens ST steam turbine SST5-3000, a three-pressure heat recovery steam generator, and a Siemens SGen5-2000H generator. Table 1 summarizes thermodynamic data of the combined cycle of the Cap Djenet plant in nominal conditions. The ambient conditions considered for nominal operation are as follows:

Temperature: 35 °C;

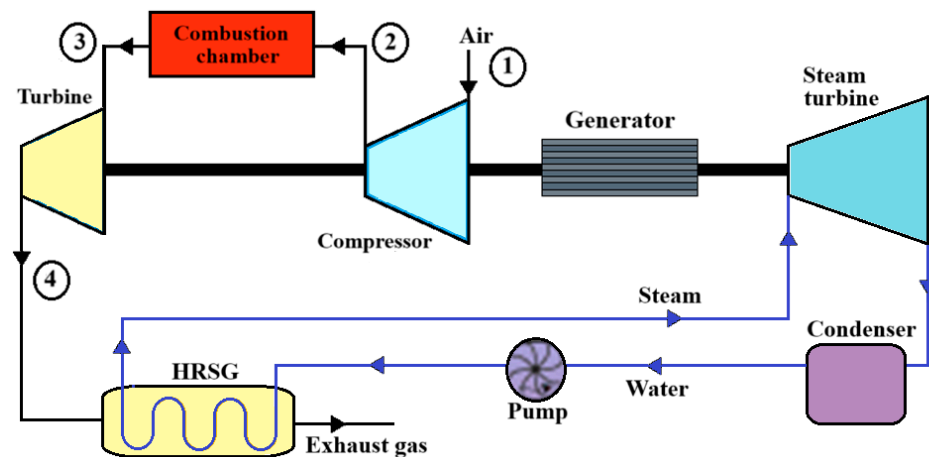
Pressure: 1.013 bar;

Relative humidity: 76%.

Our study focuses on modeling the gas turbine within the combined cycle of the power plant. Figure 1 illustrates the arrangement of the gas turbines in the combined cycle. Each of the three power plant units includes a Siemens SGT5-4000F gas turbine. The Siemens SGT5-4000F gas turbine is a single-shaft turbine consisting of a high-efficiency 15-stage axial compressor, an annular combustion chamber with 24 hybrid burners (natural gas and fuel), and a 4-stage expansion turbine coupled to a Siemens SGen5-2000H generator. Table 2 provides the performance data of the gas turbines under nominal conditions.

**Table 1.** Thermodynamic nominal data of the combined cycle of the Cap Djenet plant.

Gas Cycle	Mass Flow (kg/s)	Temperature (°C)	Pressure (bar)	Power (MW)
Air flow at compressor inlet	601.90	35.0	0.987	
Gas flow at turbine outlet	616.20	607.6	1.017	
Gas cycle power output				249.2
<b>HRSG</b>				
Gas flow at HRSG inlet	616.20	607.6	1.015	
Gas flow at HRSG outlet	616.20	90.42	1.003	
Heat output of HRSG				358.5
<b>Steam Cycle</b>				
Steam flow at HP turbine inlet	71.99	565.02	117.92	
Steam flow at IP turbine inlet	71.99	564.94	29.10	
Steam flow at LP turbine outlet	98.25	33.37	0.0514	
Steam cycle power output				127.8
<b>Combined Cycle</b>				
Power output (1 block)				377
Total power output (×3 blocks)				1131

**Figure 1.** Schematic diagram of the main elements of a gas-combined cycle.**Table 2.** Nominal data of Siemens gas turbine SGT5-4000F.

Description	Unit	Value
Grid frequency	(Hz)	50
Gas turbine power output	(MW)	249.2
Gas turbine efficiency	(%)	38.7
Fuel gas flow	(kg/s)	14.3
Exhaust temperature	(°C)	607.6
Exhaust mass flow	(kg/s)	616.2
Pressure ratio		18.8

### 3. Thermodynamic Modeling

The gas turbine's thermodynamic modeling consists of applying mass and energy equilibrium equations. This modeling aims to develop a thermodynamic model determining the performance of the gas turbine, which includes the flow of air entering the compressor as a function of atmospheric conditions.

The determination of the useful power and thermal efficiency of the gas turbine are obtained using the following equations.

Calculation of air temperature at compressor and expansion turbine outlet:

$$T_2 = T_1 + \frac{T_{2is} - T_1}{\eta_{Cis}} = T_1 \left[ 1 + \frac{\tau_C^{\frac{\gamma-1}{\gamma}} - 1}{\eta_{Cis}} \right] \quad (1)$$

$$T_4 = T_3 - \frac{T_3 - T_{4is}}{\eta_{Tis}} = T_3 \left[ 1 - \frac{1 - \left(\frac{1}{\tau_T}\right)^{\frac{\gamma-1}{\gamma}}}{\eta_{Tis}} \right] \quad (2)$$

$T_{2is}, T_{4is}$ : isentropic outlet temperature (compressor, turbine);

$\eta_{Cis}, \eta_{Tis}$ : isentropic efficiency;

$\tau_C, \tau_T$ : pressure ratio.

Equations (3) and (4) give the work per unit of mass  $W_C$  of the compressor and  $W_T$  of the turbine, respectively. The pumping work spent to evacuate the burned gases into the atmosphere is very small (less than 1% of the gas turbine's work), so its impact on the accuracy of the calculations is very low. For this reason, it was considered negligible.

$$W_C = h_2 - h_1 = C_{Pair} (T_2 - T_1) \quad (3)$$

$$W_T = h_3 - h_4 = C_{Peg} (T_3 - T_4) \quad (4)$$

$C_{Pair}$ : isobaric thermal capacity of air (kJ/kg.K);

$C_{Peg}$ : isobaric thermal capacity of exhaust gas (kJ/kg.K).

The thermal power provided by combustion is calculated as follows:

$$\dot{Q}_{CC} = \dot{m}_f PCI \quad (5)$$

$\dot{m}_f$ : mass fuel flow rate (kg/s).

The useful power of the turbine is calculated from the work of the compressor and the expansion turbine. In a steady state, the following relationship may be used:

$$\dot{W}_{GT} = \dot{m}_{eg} W_T - \dot{m} W_c \quad (6)$$

$\dot{m}_{eg}$ : mass exhaust gas flow rate (kg/s);

$\dot{m}$ : mass air flow rate (kg/s).

The thermal efficiency of a gas turbine is defined as the ratio between the useful power developed and the calorific power provided by combustion:

$$\eta_{GT} = \frac{\dot{W}_{GT}}{\dot{Q}_{CC}} \quad (7)$$

Calculating a gas turbine's power and thermal efficiency under steady-state operation requires knowledge of the compressor inlet's pressure, temperature, relative humidity,

and air mass flow rate. It is also necessary to know the rotational speed, the IGV opening angle, and the mass flow rate of the fuel. When the turbine operates under partial load and steady-state conditions, characteristic maps for the compressor and expansion turbine must also be available. These characteristic maps allow the determination of the pressure ratios and isentropic efficiencies for the compressor and expansion turbine, which are also required for the calculation.

In this paper, the study in off-design operation is limited to steady-state operation. The gas turbine, used for electricity generation, operates with a constant rotational speed fixed at a specific value (in this case, 3000 rpm). The formulations are, therefore, designed for a constant rotational speed; however, they can be adapted for different rotational speeds if the corresponding data are available. The behavior of the compressor and expansion turbine is simulated using semi-empirical thermodynamic models. These mathematical models have been calibrated for the SGT5-4000F gas turbine using data collected at the power plant. The properties of gases ( $C_p$  and  $h = C_p T$ ) are provided by temperature-dependent logarithmic polynomials according to Lanzafame Rosario [13], as follows:

$$C_p = a_0 + a_1 \ln(T^*) + a_2 \ln(T^*)^2 + a_3 \ln(T^*)^3 + a_4 \ln(T^*)^4 + a_5 \ln(T^*)^5 \quad (8)$$

$C_p$ : Isobaric thermal capacity in J/mol.K;

$T^* = T/T_0$ :  $T$  en Kelvin,  $T_0 = 298.15$  K.

The values of the coefficients  $a_0, \dots, a_5$  for the gases involved in the cycle are given in Table 3, as presented by Lanzafame Rosario [13].

**Table 3.** Logarithmic polynomial coefficients for  $C_p$  ( $100 \leq T \leq 5000$  K).

Species	$a_5$	$a_4$	$a_3$	$a_2$	$a_1$	$a_0$
O <sub>2</sub>	0.06180721	−0.15731959	−0.46630845	1.94145005	2.70119522	29.51785250
N <sub>2</sub>	0.21448719	−1.19546050	1.08309312	2.86102669	−0.21824417	28.87396814
H <sub>2</sub>	−0.15719883	0.59756168	0.01975705	−0.16827168	1.14285222	28.45084504
Ar	0.00000000	0.00000000	0.00000000	0.00000000	0.00000000	20.78600000
H <sub>2</sub> O	0.14904476	−1.35853914	2.19675399	4.39059147	0.30777852	33.36570240
CO <sub>2</sub>	0.09995132	0.00042527	−2.46535403	3.28070636	13.60436265	37.10227658

### 3.1. Mass Flow Rate of Air Entering the Axial Compressor

The following relation gives the intake air mass flow rate  $\dot{m}$  in the compressor:

$$\dot{m} = \rho q_V \quad (9)$$

When the turbine is operating at a steady state, the mass flow rate can be considered constant along the compressor. In the case of power plants, the compressor rotation speed must be kept as constant as possible so the volumetric flow  $q_V$  of air can be considered constant through a given passage section [14]. The volume flow of air varies with the variation in the angle of opening of the IGV; this variation can be considered as linear [15] according to Equation (10):

$$q_V = k \alpha_{IGV} + b \quad (10)$$

Let  $IGV = \frac{\alpha_{IGV}}{\alpha_{IGV\_MAX}}$ , the ratio of the IGV opening angle under the considered operating condition to the maximum opening angle  $\alpha_{IGV\_MAX}$  at nominal operation (100% load).

Under nominal operating conditions ( $\dot{m} = \dot{m}_0$ ;  $q_v = q_{v0}$ ;  $IGV = 1$ ), Equation (11) is obtained as:

$$\dot{m} = \rho [a (IGV - 1) + q_{v0}] \quad (11)$$

The constant coefficient “a” ( $a = k \alpha_{IGV \text{ MAX}}$ ) is determined based on data collected under nominal operating conditions and for various IGV opening angle values.

Assuming air to be a perfect gas and expressing the air density relative to its value under nominal conditions, Equation (12) is then obtained. This equation provides the mass flow rate of air entering the compressor as a function of pressure, temperature, air relative humidity, and the IGV opening angle percentage.

$$\dot{m} = \frac{M}{M_0} \frac{P}{P_0} \frac{T_0}{T} \dot{m}_0 [(a/q_{v0}) (IGV - 1) + 1] \quad (12)$$

Let the dry air have a constant average composition according to the CIPM-2007 [16], where components in very small quantities are neglected [Table 4].

**Table 4.** Composition of the dry reference air.

Component	Molar Mass (g/mol)	Molar Fraction
N <sub>2</sub>	28.0134	0.78085
O <sub>2</sub>	31.9988	0.20939
Ar	39.9480	0.00934
CO <sub>2</sub>	44.0100	0.00042

The molar mass of the ambient moist air is calculated using the saturation pressure ( $P_s$ ) given by the IAPWS 1997 industrial formula for the thermodynamic properties of water and steam [17]:

$$P_s = A_0 + A_1 T + A_2 T^2 + A_3 T^3 + A_4 T^4 + A_5 T^5 + A_6 T^6 \quad (13)$$

$A_0 = -1.7139186035 \times 10^1$ ,  $A_1 = 3.0961739394 \times 10^{-1}$ ,  $A_2 = -2.1566592224 \times 10^{-3}$ ,  $A_3 = 6.7915334500 \times 10^{-6}$ ,  $A_4 = -6.7999635030 \times 10^{-9}$ ,  $A_5 = -1.0518480668 \times 10^{-11}$ ,  $A_6 = 2.1477192075 \times 10^{-14}$ .

Equations (14) and (15) provide the molar fractions of steam and dry air in the moist air. Equations (16) and (17) provide the molar masses of dry and moist air, respectively.

$$Y_{st} = H_r \cdot \frac{P_s}{P} \quad (14)$$

$$y_{as} = 1 - y_{st} \quad (15)$$

$$M_{as} = Y_{N_2s} M_{N_2} + Y_{O_2s} M_{O_2} + Y_{Ar_s} M_{Ar} + Y_{CO_2s} M_{CO_2} \quad (16)$$

$$M = Y_{H_2O} M_{H_2O} + Y_{as} M_{as} = \frac{H_r P_s}{P} (M_{H_2O} - M_{as}) + M_{as} \quad (17)$$

From the preceding equations and Equation (12), we obtain the very interesting Equation (18), which gives the mass flow rate of air entering the compressor as a function of pressure, the ambient temperature and relative humidity, and as a function of the percentage of the IGV angle opening.

$$\dot{m} = \frac{H_r P_s (M_{H_2O} - M_{as}) + P M_{as}}{T} \frac{T_0}{P_0 M_0} \dot{m}_0 [(a/q_{v0}) (IGV - 1) + 1] \quad (18)$$

Equation (18) is very useful and practical since it allows us to directly calculate the mass flow rate of air entering the compressor for any stationary operating state of the gas turbine. It is clear that for this calculation, it is sufficient to know only the pressure, temperature, and relative humidity of the ambient air, the angle of opening of the IGV as well as the nominal operating conditions. The volume flow of air entering the compressor varies linearly with respect to the IGV opening angle according to [15]; however, an analysis of the measurements shows that this linearity is valid only over a limited range of the variation in the angle of opening of the IGV. A variation of the second degree, as presented by Equation (19), is proposed to improve the accuracy of the calculations.

$$\dot{m} = \frac{H_r P_S (M_{H_2O} - M_{as}) + P M_{as}}{T} \frac{T_0}{P_0 M_0} \dot{m}_0 [(a_1 \text{IGV}^2 + a_2 \text{IGV} + a_3)] \quad (19)$$

$a_1$ ,  $a_2$  and  $a_3$  are constants for the gas turbine Siemens SGT5-4000F:

$$a_1 = -0.2474, a_2 = 0.6784, a_3 = 0.6130.$$

It is common practice to use the air-corrected mass flow ratio to its corrected nominal value to obtain an accurate assessment. This ratio considers temperature and pressure variations and normalizes the flow rate to nominal conditions. This value is calculated as follows:

$$\dot{m}_{corr} = \frac{\dot{m}_{air} \sqrt{\frac{T_{ref}}{T}} \frac{P}{P_{ref}}}{\dot{m}_{air,0} \sqrt{\frac{T_{ref}}{T_0}} \frac{P_0}{P_{ref}}} \quad (20)$$

### 3.2. Pressure Losses

- Pressure losses at the gas turbine inlet

As it passes through the filter and the diffuser of the axial compressor, the air undergoes a pressure drop, the magnitude of which decreases under partial load operation compared to nominal operation [18]. Based on the measured values, Equation (21) is proposed to calculate the pressure losses at the compressor inlet, taking into account the air mass flow rate and density.

$$\Delta P1 = 0.73 \times \Delta P1_0 \left( \frac{\rho_0}{\rho} \right) \left( \frac{\dot{m}_{corr}}{\dot{m}_{0,corr}} \right)^2 \quad (21)$$

- Pressure losses in the combustion chamber

In off-design operation, the combustion chamber pressure losses can be expressed as a function of mass flow rate and nominal operating values [19]. The measurements show that the variation of the angle of the opening of IGVs affects the value of these pressure losses. Equation (22) is proposed to estimate the pressure losses from the corrected mass flow rate and the IGV opening angle.

$$\Delta P3 = \Delta P3_0 \left( \frac{\dot{m}_{0,corr}}{\dot{m}_{corr}} \right) (b_1 \text{IGV}^2 + b_2 \text{IGV} + b_3) \quad (22)$$

$$b_1 = -0.79, b_2 = 10.18, b_3 = 5.88.$$

### 3.3. Compression Ratios and Isentropic Efficiencies

The compressors and expansion turbines' characteristic maps are used to determine partial-load gas turbines' compression ratios and isentropic efficiency. However, since these characteristic maps are rarely available, they are often mapped; that is to say, a known

characteristic map (for example, of a compressor) is scaled up so that it corresponds, as precisely as possible, to the characteristic of the compressor in question [19,20]. We opted for semi-empirical relations based on measured data to ensure that our model retains the computational speed and flexibility, facilitating its integration into control environments or fault detection systems for gas turbines. It has been verified that these relations enable the operational matching of the compressor and the expansion turbine based on the mass flow rate.

Operating in off-design, the pressure ratios of the compressor and the expansion turbine depend on the mass flow rate of air and rotational speed [21]. The SGT5-4000F gas turbine compressor has input guide blades (IGVs); the IGV opening angle variation affects the pressure ratio value. Based on the nominal operating values, we have proposed the following equations.

$$\tau_C = (c_1 \text{IGV} + c_2) \left[ 1 - \frac{c_3}{2C_{P1}T_1} \right]^{\frac{\gamma-1}{\gamma}} \quad (23)$$

$$c_1 = 0.43, c_2 = 0.606, c_3 = 2 C_{P1,0} T_{1,0} \left( 1 - \tau_{C0}^{\frac{\gamma}{\gamma-1}} \right).$$

$$\tau_T = (d_1 \text{IGV} + d_2) \left[ 1 - \frac{d_3}{2C_{P3}T_3} \right]^{\frac{\gamma-1}{\gamma}} \quad (24)$$

$$d_1 = 19.125, d_2 = 14.625, d_3 = 2C_{P3,0} T_{3,0} \left( 1 - \tau_{T0}^{\frac{\gamma}{\gamma-1}} \right).$$

Similarly, operating in off-design, the isentropic efficiency values of the compressor and expansion turbine vary when gas mass flow rate and rotational speed vary [22]. The following proposed equations, which consider the influence of the IGV angle opening, were used.

$$\eta_C = \eta_{C0} \left( \frac{\dot{m}_{0,corr}}{\dot{m}_{corr}} \right) (e_1 \text{IGV}^2 + e_2 \text{IGV} + e_3) \quad (25)$$

$$\eta_T = \eta_{T0} \left( \frac{\dot{m}_{0,corr}}{\dot{m}_{corr}} \right) (e_1 \text{IGV}^2 + e_3 \text{IGV} + e_3) \quad (26)$$

$$e_1 = -0.15, e_2 = 0.60, e_3 = 0.52.$$

#### 4. Validation and Results of Models

The mathematical models proposed in this study were verified by comparing them with measurements made at the plant. Four series of measurements were taken, each for a fixed IGV opening angle for different air intake atmospheric conditions. The comparison of the results obtained by the proposed model with the data collected at the plant level shows very good calculation precision.

The mass flow rate of air entering the gas turbine compressor is the first area of interest. The prediction of the value of this flow rate is the essential element of our study; Figure 2 shows the measured and calculated values of the corrected mass flow rate of air entering the compressor for different atmospheric conditions and IGV opening angle according to the proposed model (Equation (19)). The comparison between simulated and measured values (Figure 3) shows that the proposed model gives very precise values, the coefficient of determination  $R^2$  is high ( $R^2 = 0.9796$ ), and the mean quadratic error RMSE is very low (RMSE = 0.0213). The model (Equation (19)) can be considered valid; this validation represents the most important result of this study. This model's accuracy was enhanced by incorporating a refined approach to the variation of the air volume flow rate at the compressor inlet. Specifically, the relationship between the volume flow rate and the angle of the inlet guide vanes (IGV) was modeled using a second-degree polynomial function

rather than a simple proportional relationship. This improvement captures the nonlinear behavior more accurately, thereby increasing the precision of the model's predictions.

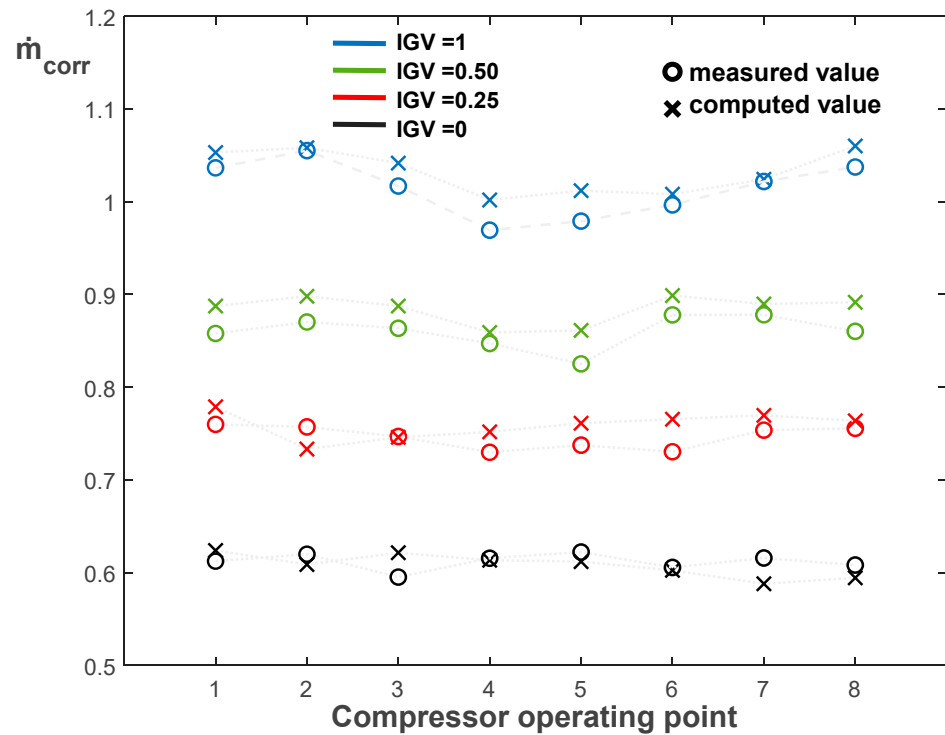


**Figure 2.** Corrected mass flow rate of air entering the compressor for different atmospheric conditions and IG V opening angles.

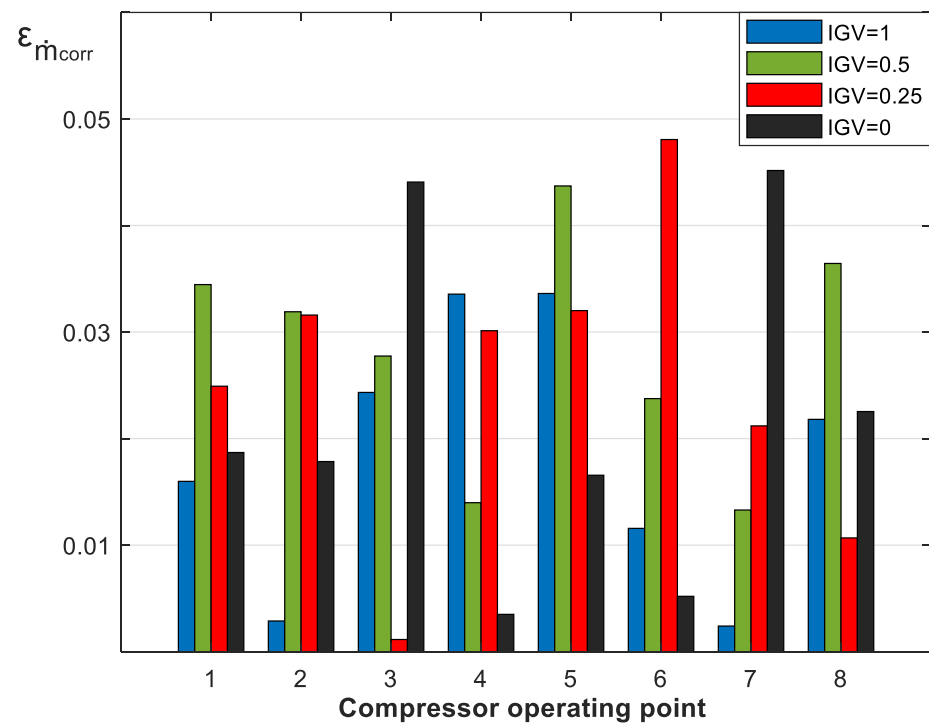


**Figure 3.** Calculation precision of the corrected mass flow rate for different operating states of the compressor.

The other proposed equations and their associated results are then examined, and Table 5 summarizes the precision achieved by the proposed models. The table gives the

average accuracy of all series values. The values of the coefficient of determination are found to be high and greater than 0.95 except for isentropic efficiency of the compressor and expansion turbine and thermal efficiency of the gas turbine. However, for the latter, the coefficient of determination is greater than 0.92 and the accuracy of the results can be considered acceptable.

**Table 5.** Average accuracy of calculated values.

Parameter Name	Designation	R <sup>2</sup>	RMSE
Corrected mass flow rate of air	$\dot{m}_{corr}$	0.9796	0.0213
Compressor pressure ratio	$\tau_C$	0.9767	0.4398
Isentropic efficiency of the compressor	$\eta_{Cis}$	0.9264	0.0116
Pressure ratio of the expansion turbine	$\tau_T$	0.9876	0.3164
Isentropic efficiency of the expansion turbine	$\eta_{Tis}$	0.9118	0.0204
Pressure drop of filter and compressor inlet	$\Delta P_1$	0.9607	0.0003
Combustion chamber pressure drop	$\Delta P_2$	0.9575	0.0156
Power of the gas turbine	$\dot{W}_{GT}$	0.9843	8.0003
Thermal efficiency of the the gas turbine	$\eta_{GT}$	0.9307	0.0117

Figure 4 compares the compressor compression ratio values calculated by the proposed model (Equation (23)) with the measured values and thus shows that these calculated values are very close to the measured values. In general, models lose some of their accuracy with the increase in the angle opening of IGVs, except for the relative error of pressure losses, which is slightly greater than 5% to approach 10% at the maximum opening of the IGV.

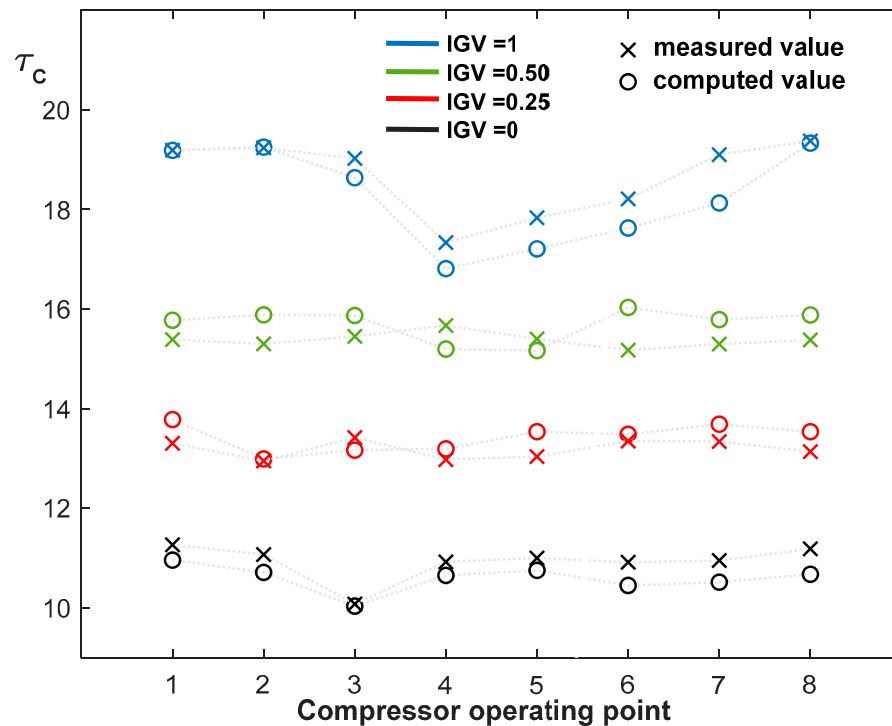


**Figure 4.** Compression ratio calculated and measured for different states of its operation.

Figure 5 shows an example of using our model, which is a prediction of the output and thermal efficiency of the gas turbine (SGT5-4000F) as a function of ambient air temperature. In this simulation, the following data were taken into account:

- The ambient pressure and relative humidity of are constant ( $P_{\text{air}} = 1.013 \text{ bar}$ ,  $H_r = 0.60$ ) by varying its temperature from  $5 \text{ }^\circ\text{C}$  to  $40 \text{ }^\circ\text{C}$ .
- The IGV aperture angle is maximum and kept constant ( $\alpha_{\text{IGV}} = 100\%$ ).
- The temperature of the gases burned at the inlet to the expansion turbine is constant ( $T_3 = \text{TIT} = 1350 \text{ K}$ ).

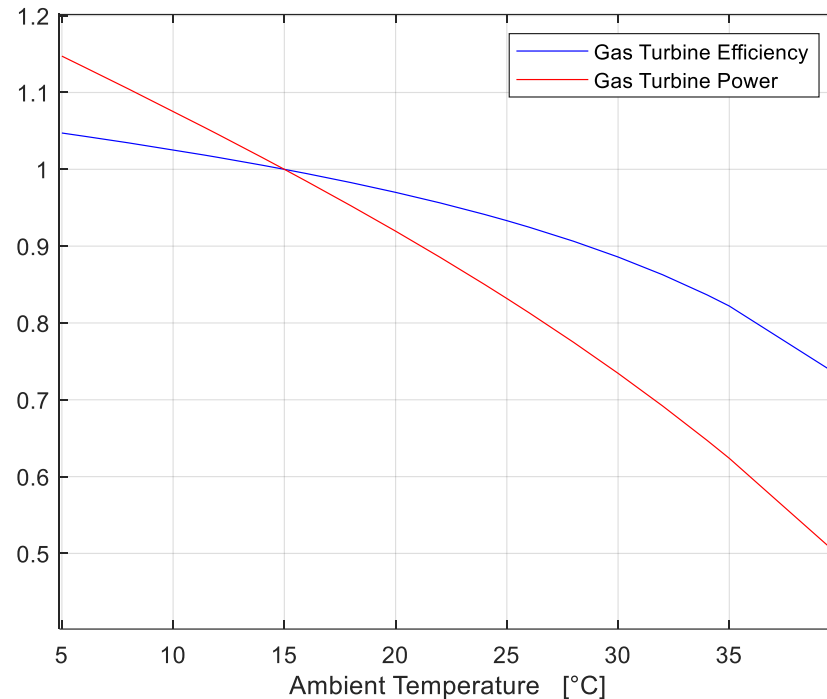


**Figure 5.** Gas turbine performance as a function of ambient temperature.

## 5. Conclusions

This study presents an advanced off-design thermodynamic model of the Siemens SGT5-4000F gas turbine, integrated into a combined cycle power plant. The model encompasses detailed representations of the axial compressor, combustion chamber, and expansion turbine, enabling precise determination of the gas turbine's net power output and thermal efficiency. Furthermore, the model incorporates key aspects such as pressure drops across the air filter and the combustion chamber.

A notable innovation of this work lies in its ability to predict gas turbine performance directly based on ambient inlet conditions—namely pressure, temperature, and relative humidity—combined with the position of the compressor inlet guide vanes (IGV).

The model's validity was demonstrated through comparative analyses against measurement data, yielding high coefficients of determination and low root mean square errors. In addition to its high accuracy, the model offers computational efficiency and relies on a minimal input data set, making it highly suitable for applications such as simulation, optimization, and fault diagnosis in complex operational scenarios.

**Author Contributions:** The work was done by the two authors, T.B. and K.M. All authors have read and agreed to the published version of the manuscript.

**Funding:** This research received no external funding.

**Data Availability Statement:** Data are contained within the article.

**Conflicts of Interest:** The authors declare no conflict of interest.

## Nomenclature

a	coefficient of variation of the volume flow per percent of the IGV opening
$C_p$	isobaric thermal capacity of gases (kJ/kg.K)
h	gas enthalpy (kJ/kg)
Hr	relative air humidity (%)
IGV	percentage of IGV opening angle (%)
$\dot{m}$	mass flow rate of gases (kg/s)
M	molar mass of wet air (g/mol)
M <sub>as</sub>	molar mass of dry air (g/mol)
M <sub>H<sub>2</sub>O</sub>	molar mass of water (g/mol)
PCI	fuel lower calorific value (kJ/kg)
P <sub>s</sub>	water saturation pressure (bar)
$\dot{Q}_{CC}$	thermal power provided by combustion
q <sub>v</sub>	volume flow rate of air (m <sup>3</sup> /s)
R <sup>2</sup>	coefficient of determination
RMSE	root mean squared error
T	gas temperature (K)
V	air flow rate (m/s)
W	work per mass unit (J/kg)
$\dot{W}_{GT}$	gas turbine useful power (W)
y <sub>as</sub>	molar fraction of dry air in wet air (%)
y <sub>st</sub>	molar fraction of water vapor in wet air (%)

### Greek letters

$\Delta P$	pressure losses (bar)
$\alpha_{IGV}$	IGV opening angle (°)
$\varepsilon$	relative error of the calculated value (%)
$\eta$	efficiency
$\eta_{GT}$	thermal efficiency of the gas turbine
$\tau$	pressure ratio
$\rho$	air density (kg/m <sup>3</sup> )

### Subscripts

0	relating to nominal operating conditions
1	compressor inlet
2	compressor outlet
3	expansion turbine inlet
4	expansion turbine outlet
air	atmospheric air
C	compressor
corr	corrected value
f	fuel
eg	exhaust gases
is	isentropic value
T	expansion turbine

## References

- Walsh, P.; Fletcher, P. *Gas Turbine Performance*, 2nd ed.; Blackwell Science: Hoboken, NJ, USA, 2004; ISBN 978-0-470-77453-3.
- Sammour, A.A.; Komarov, O.V.; Lattieff, F.A.; Qasim, M.A.; Saleh, A.Y. Influence of Surrounding Air Temperature and Humidity upon the Performance of a Gas Turbine Power Plant. *J. Adv. Res. Fluid Mech. Therm. Sci.* **2023**, *112*, 22–37. [[CrossRef](#)]
- Alaabidy, W.H.S.; Antipov, Y.A.; Al-Rubaiawi, M.S.S.A.-R.; Frolov, M. Gas Turbine Suitable for the Ambient Conditions Prevailing in Arab Gulf Countries—A Prognostic Analysis. *J. Appl. Eng. Sci.* **2023**, *21*, 982–998. [[CrossRef](#)]
- Ibrahim, T.K.; Basrawi, F.; Awad, O.I.; Abdullah, A.N.; Najafi, G.; Mamat, R.; Hagos, F. Thermal Performance of Gas Turbine Power Plant Based on Exergy Analysis. *Appl. Therm. Eng.* **2017**, *115*, 977–985. [[CrossRef](#)]

5. Facchini, B.; Fiaschi, D.; Manfrida, G. Exergy and exergo-economic based analysis of a gas turbine power generation system. *J. Power Technol.* **2013**, *93*, 44–51. [[CrossRef](#)]
6. González-Díaz, A.; Alcaráz-Calderón, A.M.; González-Díaz, M.O.; Méndez-Aranda, Á.; Lucquiaud, M.; González-Santaló, J.M. Effect of the ambient conditions on gas turbine combined cycle power plants with post-combustion CO<sub>2</sub> capture. *Energy* **2017**, *134*, 221–233. [[CrossRef](#)]
7. Hashmi, M.B.; Lemma, T.A.; Karim, Z.A.A. Investigation of the Combined Effect of Variable Inlet Guide Vane Drift, Fouling, and Inlet Air Cooling on Gas Turbine Performance. *Entropy* **2019**, *21*, 1186. [[CrossRef](#)]
8. Fang, J.; Wang, R. Influence of IGV Opening Degree on the Compressor Efficiency of MITSUBISHI F4 Gas Turbine. *Power Gener. Technol.* **2020**, *41*, 317. [[CrossRef](#)]
9. Ricci, M.; Benvenuto, M.; Mosele, S.G.; Pacciani, R.; Marconcini, M. Predicting the Impact of Compressor Flexibility Improvements. *Energies* **2022**, *15*, 7546. [[CrossRef](#)]
10. Zhu, W.; Ren, X.; Li, X.; Gu, C.; Liu, Z.; Yan, Z.; Zhu, H.; Zhang, T. Improvement of part-load performance of gas turbine by adjusting compressor inlet air temperature and IGV opening. *Front. Energy* **2022**, *16*, 1000–1016. [[CrossRef](#)]
11. Purba, O.; Zhultriza, F. Inlet Guide Vane Tracking Effectiveness at Various Compressor Efficiency of Gas Turbine. *IOP Conf. Ser. Mater. Sci. Eng.* **2021**, *1096*, 012088. [[CrossRef](#)]
12. Wang, Z.; Duan, L. Thermo-economic Optimization of Steam Pressure of Heat Recovery Steam Generator in Combined Cycle Gas Turbine under Different Operation Strategies. *Energies* **2021**, *14*, 4991. [[CrossRef](#)]
13. Rosario, L. Thermodynamic Property Models for Unburned Mixtures and Combustion Gases. *Int. J. Thermodyn.* **2006**, *9*, 73–80.
14. Pourhedayat, S.; Hu, E.; Chen, L. An improved semi-analytical model for evaluating performance of gas turbine power plants. *Energy* **2023**, *267*, 126583. [[CrossRef](#)]
15. Trawiński, P. Development of flow and efficiency characteristics of an axial compressor with an analytical method including cooling air extraction and variable inlet guide vane angle. *Arch. Thermodyn.* **2021**, *42*, 17–46. [[CrossRef](#)]
16. Picard, A.; Davis, R.S.; Gläser, M.; Fujii, K. Revised formula for the density of moist air (CIPM-2007). *Metrologia* **2008**, *45*, 149–155. [[CrossRef](#)]
17. Wagner, W.; Cooper, J.R.; Dittmann, A.; Kijima, J.; Kretschmar, H.-J.; Kruse, A.; Mareš, R.; Oguchi, K.; Sato, H.; Stöcker, I.; et al. The IAPWS Industrial Formulation 1997 for the Thermodynamic Properties of Water and Steam. *J. Eng. Gas Turbines Power* **2000**, *122*, 150–182. [[CrossRef](#)]
18. Lee, J.J.; Kang, D.W.; Kim, T.S. Development of a gas turbine performance analysis program and its application. *Energy* **2011**, *36*, 5274–5285. [[CrossRef](#)]
19. Payri, F.; Serrano, J.; Fajardo, P.; Reyes-Belmonte, M.; Gozalbo-Belles, R. A physically based methodology to extrapolate performance maps of radial turbines. *Energy Convers. Manag.* **2012**, *55*, 149–163. [[CrossRef](#)]
20. Zhang, Y.; Liu, P.; Li, Z. Gas turbine off-design behavior modelling and operation windows analysis under different ambient conditions. *Energy* **2023**, *262*, 125348. [[CrossRef](#)]
21. Zhang, N.; Cai, R. Analytical solutions and typical characteristics of part-load performances of single shaft gas turbine and its cogeneration. *Energy Convers. Manag.* **2002**, *43*, 1323–1337. [[CrossRef](#)]
22. Dias, F.L.G.; Nascimento, M.A.R.D.; Rodrigues, L.D.O. Reference Area Investigation in a Gas Turbine combustion chamber using CFD. *J. Mech. Eng. Autom.* **2014**, *4*, 73–82. [[CrossRef](#)]

**Disclaimer/Publisher’s Note:** The statements, opinions and data contained in all publications are solely those of the individual author(s) and contributor(s) and not of MDPI and/or the editor(s). MDPI and/or the editor(s) disclaim responsibility for any injury to people or property resulting from any ideas, methods, instructions or products referred to in the content.